

## Werk

**Jahr:** 1974

**Kollektion:** fid.geo

**Signatur:** 8 Z NAT 2148:40

**Digitalisiert:** Niedersächsische Staats- und Universitätsbibliothek Göttingen

**Werk Id:** PPN1015067948\_0040

**PURL:** [http://resolver.sub.uni-goettingen.de/purl?PPN1015067948\\_0040](http://resolver.sub.uni-goettingen.de/purl?PPN1015067948_0040)

**LOG Id:** LOG\_0096

**LOG Titel:** The neural atmosphere temperature experiment

**LOG Typ:** article

## Übergeordnetes Werk

**Werk Id:** PPN1015067948

**PURL:** <http://resolver.sub.uni-goettingen.de/purl?PPN1015067948>

**OPAC:** <http://opac.sub.uni-goettingen.de/DB=1/PPN?PPN=1015067948>

## Terms and Conditions

The Goettingen State and University Library provides access to digitized documents strictly for noncommercial educational, research and private purposes and makes no warranty with regard to their use for other purposes. Some of our collections are protected by copyright. Publication and/or broadcast in any form (including electronic) requires prior written permission from the Goettingen State- and University Library.

Each copy of any part of this document must contain these Terms and Conditions. With the usage of the library's online system to access or download a digitized document you accept the Terms and Conditions.

Reproductions of material on the web site may not be made for or donated to other repositories, nor may be further reproduced without written permission from the Goettingen State- and University Library.

For reproduction requests and permissions, please contact us. If citing materials, please give proper attribution of the source.

## Contact

Niedersächsische Staats- und Universitätsbibliothek Göttingen  
Georg-August-Universität Göttingen  
Platz der Göttinger Sieben 1  
37073 Göttingen  
Germany  
Email: [gdz@sub.uni-goettingen.de](mailto:gdz@sub.uni-goettingen.de)

# The Neutral Atmosphere Temperature Experiment

N. W. Spencer, D. T. Pelz, H. B. Niemann

Goddard Space Flight Center

G. R. Carignan, J. R. Caldwell

University of Michigan

Received July 2, 1974

*Abstract.* The AEROS Neutral Atmosphere Temperature Experiment (NATE) is designed to measure the kinetic temperature of molecular nitrogen ( $N_2$ ) in the thermosphere. A quadrupole mass spectrometer tuned to  $N_2$  measures the  $N_2$  density variation in a small spherical antechamber having a knife-edged orifice which is exposed to the atmosphere at the outer surface of the spacecraft. The changing density of  $N_2$  due to the spinning motion of the spacecraft permits determination of the velocity distribution of the  $N_2$  from which the temperature is calculated. An alternate mode of operation of the instrument allows measurement of the other gases in the atmosphere as well as  $N_2$  permitting determination of the neutral particle composition of the atmosphere.

*Key words:* Neutral Atmosphere Temperature — Kinetic Temperature — Molecular Nitrogen Density — Velocity Distribution Analyzer — Thermosphere Composition — Neutral Gas Mass-spectrometer.

## Introduction

The objective of the Neutral Atmosphere Temperature Experiment (NATE) on the AEROS satellite is to provide *in situ* measurements of (a) the kinetic temperature of molecular nitrogen in the thermosphere, (b) the molecular-nitrogen density, and (c) the total neutral gas density, to aid in the study of aeronomy. The basis of the experimental approach to temperature determination is measurement of the velocity distribution of the atmospheric molecular nitrogen molecules, which can be interpreted as the kinetic temperature.

A quadrupole mass spectrometer is used to select molecular nitrogen for the temperature measurement. Periodically it is configured to measure the concentrations of the other atmospheric gases which permits a determination of the total density.

## Principle and Application of the Method

The number density of a gas of mass  $m$  within a moving enclosure (antechamber) that is open to the atmosphere through a knife-edged orifice with an area small compared to the antechamber surface area can

be expressed by the following Eq. (Tsien, 1946; Schultz, Spencer, and Reifman, 1948; Spencer, Boggess, LaGow, and Horowitz, 1959; Spencer, Brace, Carignan, Tausch, and Niemann, 1965; Spencer, Niemann, and Carignan, 1973):

$$N_i = N_a (T_a/T_i)^{1/2} f(s \cos \alpha) \quad (1)$$

where

- $N_i$  = instantaneous density of the gas in the antechamber;
- $N_a$  = ambient density of the gas;
- $T_a$  = ambient temperature of the gas;
- $T_i$  = temperature of the gas in the antechamber;
- $s$  =  $V / \sqrt{2kT_a/m}$  = ratio of antechamber velocity to most probable thermal velocity of the ambient gas particles;
- $V$  = speed of the antechamber with respect to the gas;
- $\sqrt{2kT_a/m}$  = most probable thermal velocity of the ambient gas particles;
- $\alpha$  = angle between the normal to the orifice plane and the satellite velocity vector;
- $i, a$  = subscripts for internal and ambient, respectively;
- $f(s \cos \alpha) = \exp(-s^2 \cos^2 \alpha) + \sqrt{\pi} s \cos \alpha (1 + \operatorname{erf}(s \cos \alpha))$ .

The equation can be solved for the difference between  $N_i$  max (minimum angle of attack) and  $N_i$  min (maximum angle of attack) to yield

$$N_a = N_i (N_i(\max) - N_i(\min)) / 2 \sqrt{\pi} s_i \cos \alpha_{\min} \quad (2)$$

thus eliminating the unknown  $T_a$ , and providing  $N_a$  the ambient density. In this equation,

$$s_i = V / (2kT_i/m)^{1/2} \quad (3)$$

In the general case, these expressions can be used as follows. Consider the antechamber to be located at the equator of a spinning spacecraft, with the orifice plane normal to a radius and facing outward. The internal gas density (in this case mass 28, ( $N_2$ )) that is observed is illustrated in Fig. 1, which is taken from San Marco 3 Omegatron data. As the component of satellite velocity that is normal to the orifice plane approaches and passes through zero ( $\alpha = 90^\circ$ ), the value of the function  $N_i$  becomes more dependent on the ambient temperature. In Fig. 1 this is the region where the curve approaches the horizontal. The density variation occurring in the antechamber in this region is reflected in the variable  $f(s \cos \alpha)$  shown in Fig. 2 where  $s \cos \alpha$  approaches zero and becomes negative. Since  $T_i$

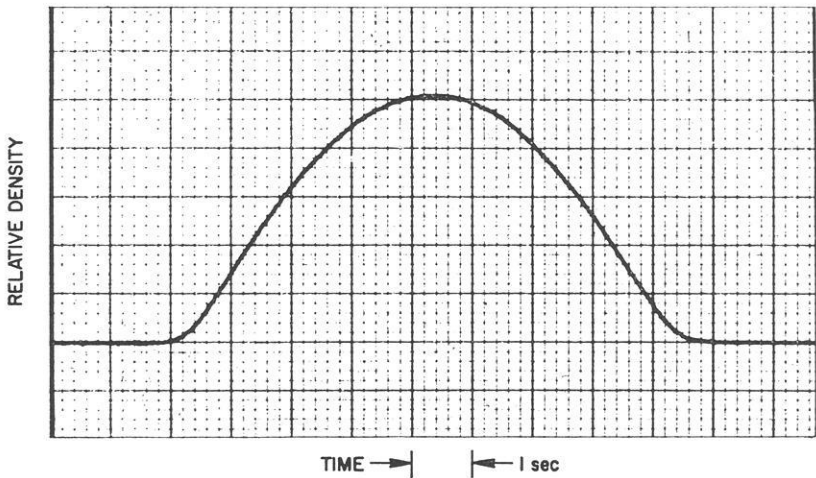


Fig. 1. Internal N<sub>2</sub> density ( $N_i$ ) observed during one spin period of the San Marco III satellite

| $s \cos \alpha$ | $f(s \cos \alpha)$ | $\alpha$ |
|-----------------|--------------------|----------|
| -2.85           | 0.000016           | 105.0    |
| -2.57           | 0.000085           | 103.5    |
| -2.29           | 0.00040            | 102.0    |
| -2.00           | 0.0017             | 100.5    |
| -1.72           | 0.006              | 99.0     |
| -1.43           | 0.019              | 97.5     |
| -1.00           | 0.054              | 96.0     |
| -0.84           | 0.144              | 94.5     |
| -0.57           | 0.291              | 93.0     |
| -0.28           | 0.570              | 91.5     |
| 0               | 1.00               | 90.0     |
| 0.28            | 1.59               | 88.5     |
| 0.57            | 2.35               | 87.0     |
| 0.86            | 3.18               | 85.5     |
| 1.15            | 4.13               | 84.0     |
| 1.44            | 5.12               | 82.5     |

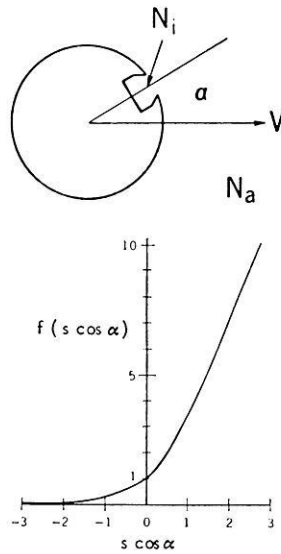


Fig. 2. Illustration of the functional relationship  $f(s \cos \alpha) = \exp(s^2 \cos^2 \alpha) + \sqrt{\pi} s \cos \alpha (1 + \text{erf}(s \cos \alpha))$

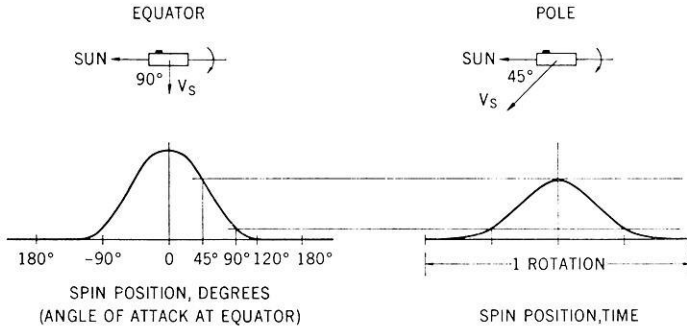


Fig. 3. Internal  $N_2$  density variation for the AEROS satellite. Two cases are shown — one corresponding to the equator crossing when the angle of attack is minimum, and the other to the maximum latitude crossing when the angle of attack is maximum

(equivalent to antechamber temperature),  $V$ , and  $\cos \alpha$  are measured and thus considered known, and  $N_a$  can be computed from Eq. (2), the temperature  $T_a$  can be calculated.

#### *AEROS Data Analysis*

The representative antechamber density ( $N_i$ ) variation as a function of spin position is shown in Fig. 3 for the two extreme cases for AEROS; when the satellite is crossing the equator and when it is passing through the maximum latitude position. The different maxima result from the changing angle between the spin axis and the satellite velocity vector (also shown in Fig. 3) a consequence of the solar pointing orientation of the satellite spin axis. The maximum values occur when the orifice plane normal is closest to the direction of motion of the satellite (between  $0^\circ$  and  $45^\circ$ ) and the  $180^\circ$  point when furthest.

The shape of the curves of Fig. 3 in the  $90^\circ$  region are significantly temperature dependent from about  $84^\circ$  to about  $105^\circ$ , the angle where the signal-to-noise ratio becomes unacceptably low. Although an analysis can be carried out by fitting a curve to the data in the  $90^\circ$  region and computing unique values of density and  $\rho \cos \alpha$  to determine the temperature, the temperature is more easily and precisely determined using a different approach. With reference to Fig. 4, the  $1500^\circ$  and  $750^\circ$  curves represents  $N_i$  for the two representative temperatures in the region near  $90^\circ$  where the temperature information exists. The  $0^\circ$  curve represents  $N_i$  for a fictitious case where  $T_i = 0$ . The temperature  $T_a$  is proportional to the area between the  $0^\circ$  curve and an actual curve. The  $90^\circ$  point, whose location must be established quite accurately to identify the correct  $0^\circ$  curve, is determined by applying the criterion that the areas to the left and right of a vertical drawn

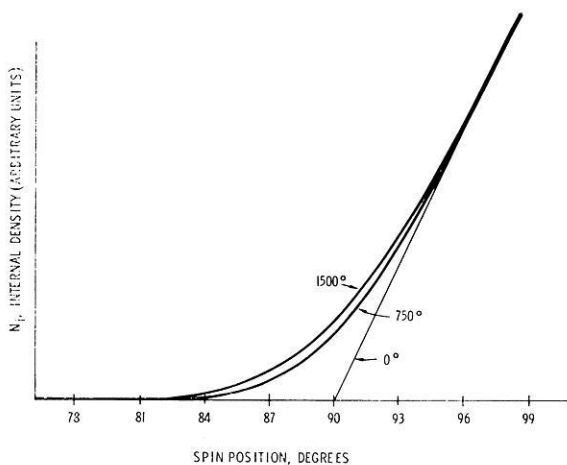


Fig. 4. Illustration of the internal  $N_2$  density variation in the  $90^\circ$  region for two typical cases, and a zero temperature case pertaining to temperature calculation. The area between any actual and the zero temperature curve is proportional to the temperature

through the  $90^\circ$  point are equal. Having done this, the area between the  $0^\circ$  and the actual curve is determined, and the temperature calculated from the area and the maximum value of the internal density, with knowledge of the angle of attack and spacecraft velocity.

#### *Instrument Description*

A quadrupole mass spectrometer whose ion source region is coupled through a high conductance path to a spherical, stainless steel antechamber is employed in the instrument (Fig. 5). The antechamber is 32 mm in diameter and the circular knife-edged orifice is 5 mm in diameter. These elements, comprising the sensor, are located at the satellite periphery on the equatorial plane as discussed previously. The sensor is baked and vacuum-sealed prior to launch, and opened to the atmosphere after the satellite is in orbit, to insure vacuum cleanliness. Because of the high conductance path between the antechamber and ion source, the number of ions produced in the ion source region is proportional to the antechamber density and hence  $N_i$ . The quadrupole analyzer is tuned to the particular ion desired (molecular nitrogen in the case of temperature measurement). Ions arriving at the first dynode of the multiplier result in pulses of electrons at the multiplier output with a rate proportional to the gas density in the ion source.

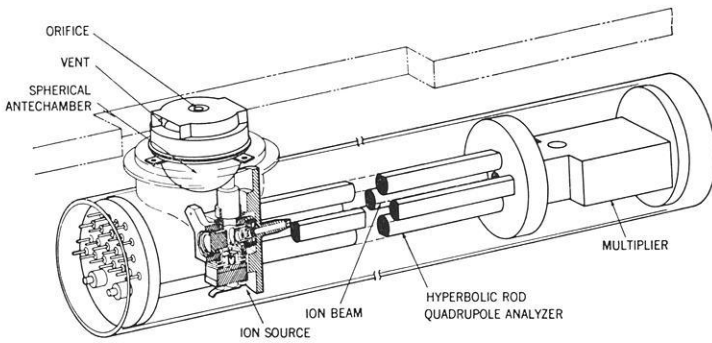


Fig. 5. Drawing of AEROS NATE sensor showing spherical antechamber and orifice, and quadrupole arrangement

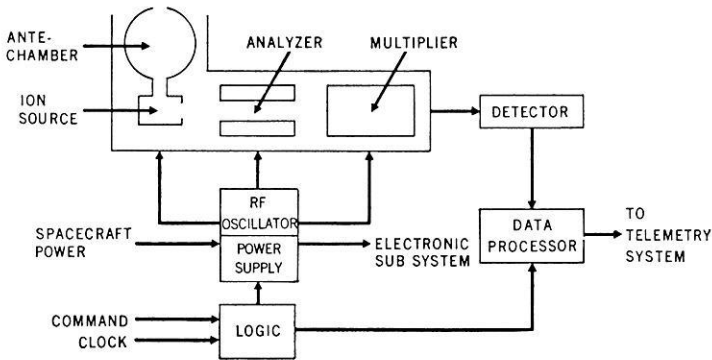


Fig. 6. Simplified block diagram of AEROS NATE instrument

The electronic system includes a pulse counter, data processor, power supplies, and logic as shown in the block diagram in Fig. 6 and in more detail in Fig. 7. The detector amplifies the multiplier output pulses for the data processor, which provides digital output signals in the proper format to the telemetry system that are proportional to the instantaneous density of neutral molecular nitrogen in the spherical antechamber. The instantaneous value of the density is sampled 44 times per spacecraft spin period with increased time resolution in the  $90^\circ$  region, as illustrated in Fig. 8 which shows the distribution of data points nominally superimposed on a typical curve of expected chamber density variation. The telemetry data frame is timed by a special spacecraft sensor which detects the direction of flow of ambient ions and causes nearly fixed phasing of the data frame and the ion stream.

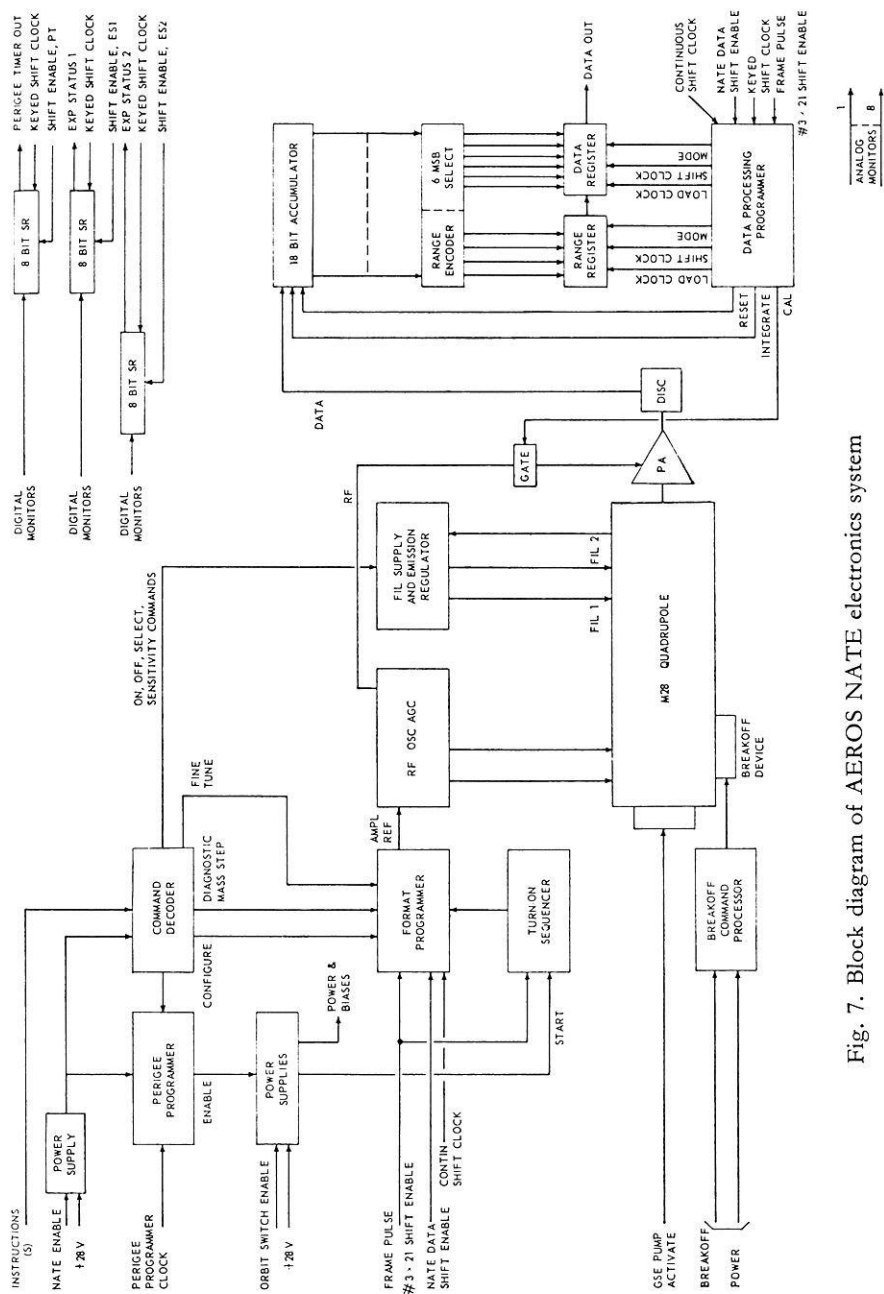


Fig. 7. Block diagram of AEROS NATE electronics system



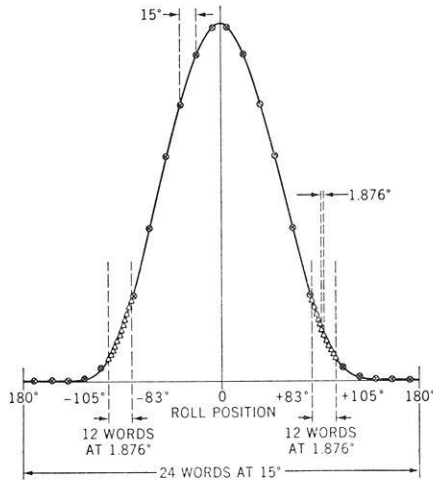


Fig. 8. Drawing of representative internal density variation for one spin cycle showing optimum location of data words

### *Instrument Performance Considerations*

The nominal altitude range of the experiment is determined at the upper limit by the signal-noise ratio of the instrument system, and at the lower limit by the maximum internal number density at which the ion source can operate satisfactorily, or by the upper limit of detection capability. Fig. 9 shows the instrument transfer function *vs.* altitude at  $\alpha = 0^\circ$  and  $\alpha = 90^\circ$  for two exospheric temperatures. The output is based on a nominal sensitivity of  $4 \times 10^{22}$  particles  $\text{cm}^{-3} \text{A}^{-1}$  for the quadrupole mass spectrometer employed.

When the number of counts measured at the electron multiplier is equal to  $1.6 \times 10^3$ , the statistical uncertainty of the count is 2.5%. This leads to a temperature uncertainty of 5% and a density uncertainty of 2.5% due to statistical limitations. It therefore sets upper altitude limits of 270 and 380 km for 5% temperature measurements and 360 and 600 km for 2.5% density measurements, depending on the exospheric temperature. The only other significant error in the measurement is due to calibration uncertainty which affects the density but not the temperature measurement.

At the lower altitudes the limit is established by the maximum count rate of  $\approx 8$  MHz ( $2^{18}$  counts per 0.03 seconds). For the nominal AEROS perigee of 235 km, the maximum output is on range for exospheric temperatures up to about 1000 °K. To be "on range" for the reentry phase and to provide some margin for the nominal orbit, the ion source sensitivity can

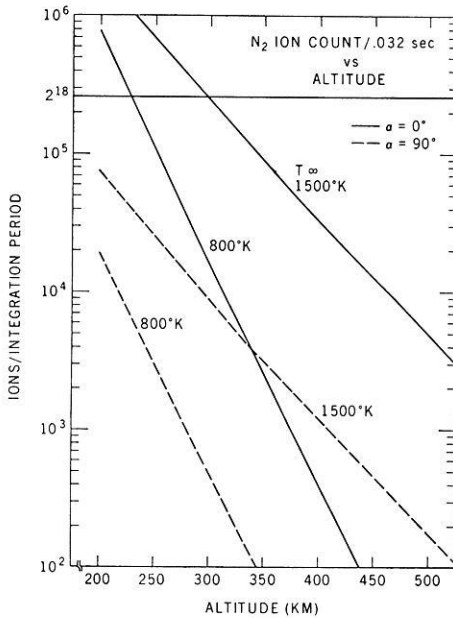


Fig. 9. Curves illustrating anticipated  $N_2$  ion count versus altitude for representative atmospheric temperatures

be reduced up to a factor of 10 on command. This will permit an extension of the lower altitude limit to less than 175 km. The range of measurement is summarized as follows:

| Exospheric Temperature | Temperature Measurement | Density Measurement |
|------------------------|-------------------------|---------------------|
| 800 °K                 | 175–270 km              | 175–360 km          |
| 1500 °K                | 175–380 km              | 175–600 km          |

There are additional factors which can affect the determination of temperature by the technique discussed here but which for AEROS are not believed to be significant. For example, at all altitudes for which AEROS measurements are expected, the mean free path is sufficiently long so that a free molecular flow assumption is quite valid. It follows that Eq. (1) can safely be applied in this regard. Another and more demanding consideration in the applicability of Eq. (1) is the question of gas-surface interactions in the antechamber and ion source. It is clearly important that the gas employed not be significantly sorbed by the walls which would inhibit free diffusion

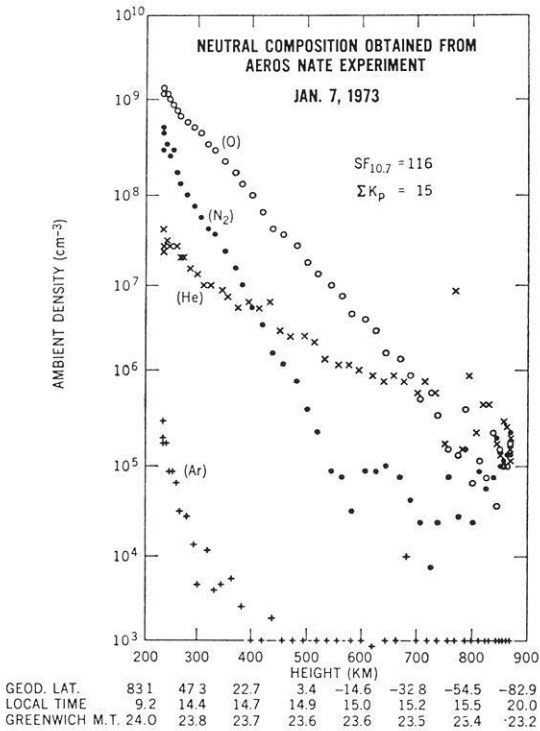


Fig. 10. Example of atmospheric neutral particle composition obtained from the AEROS 1 NATE experiment. The wave-like structure observable in the curves at lower altitudes reflect true atmospheric variations. The scattering of data points to be seen at the highest altitudes reflect telemetry noise and illustrate the altitude limit of the instrument due to the noise

of the internal gas and the atmosphere. This condition is readily attained with the non-reactive gases argon, helium and nitrogen. Nitrogen was selected and is most useful for AEROS because of its relatively large concentration. Its very small surface affinity is negligible at all altitudes where temperature measurement is possible with AEROS.

#### *In Orbit Performance of the Instrument*

The NATE instrument was flown on the first AEROS satellite and functioned correctly from initial turn-on until reentry. Because of a difficulty in the ion stream detection system of the spacecraft, proper synchronism of the data frame with the spin position was not routinely achieved. As a consequence, the high density of data points expected in the  $90^\circ$  region was

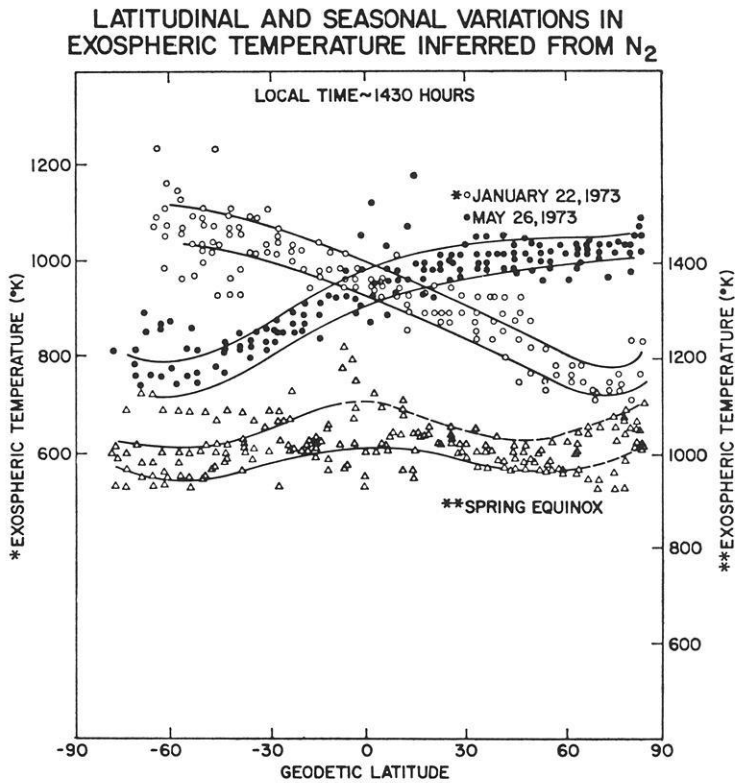


Fig. 11. Exospheric temperature data inferred from N<sub>2</sub> density obtained by the AEROS 1 NATE instrument

not realized, and thus temperature measurement by the technique discussed above could not be carried out. However, the instrument was operated in an alternate mode to provide atmospheric composition throughout the mission. Representative data obtained are shown in Fig. 10. The wave-like structure seen in the curves results from true atmospheric variations, however, the large scatter in data points at the higher altitudes does not of course reflect the atmosphere, but illustrates the altitude limit of the instrument due to noise.

The measured density permits the determination of an inferred temperature. This has been done with some of the molecular nitrogen data obtained, and a typical result is shown in Fig. 11. Assuming diffusive equilibrium and the lower boundary temperature, each density value can be interpreted as a temperature. The data were selected for three times of the year to illustrate the annual variation of exospheric temperature.

*Acknowledgement.* We recognize and wish to note here the significant contributions to the design, development and the implementation of the NATE experiment by many individuals at Goddard Space Flight Center and the University of Michigan. In particular, we acknowledge the special efforts of J. J. L'Eplattenier and Plymouth Freed at the University and H. Benton, R. Abell, H. Powers and Dr. W. Kasprzak at GSFC. The contributions of R. Theis, L. Purves, Dr. W. Hoegy, and L. Wharton to data analysis are noted with pleasure. We also express our appreciation to the AEROS Project personnel for their help in accommodating our experiment.

### *References*

- Schultz, F. V., Spencer, N. W., Reifman, A.: Upper Air Research Program Report 2, Engineering Research Institute, University of Michigan, July 1, 1948, Air Material Command, Cambridge Field Station
- Spencer, N. W., Boggess, R. L., LaGow, H. E., Horowitz, R.: On the use of ionization gage devices at very high altitudes. *Am. Rocket Soc. J.* 29, 290, 1959
- Spencer, N. W., Brace, L. H., Carignan, G. R., Tausch, D. R., Niemann, H.: Electron and molecular nitrogen temperature and density in the thermosphere. *JGR* 70, 2665, 1965
- Spencer, N. W., Niemann, H. B., Carignan, G. R.: The neutral-atmosphere temperature instrument. *Radio Sci.* 8, 287, 1973
- Tsien, H.: Superaerodynamics. *J. Aeron. Sci.* 13, 653, 1946

N. W. Spencer  
Code 620  
Laboratory for Planetary Atmospheres  
Goddard Space Flight Center  
Greenbelt, Md. 20771  
USA